CASE FILE COPY NACA

RESEARCH MEMORANDUM

VELOCITY DISTRIBUTIONS MEASURED IN THE SLIPSTREAM OF
EIGHT-BLADE AND SIX-BLADE DUAL-ROTATING

PROPELLERS AT ZERO ADVANCE

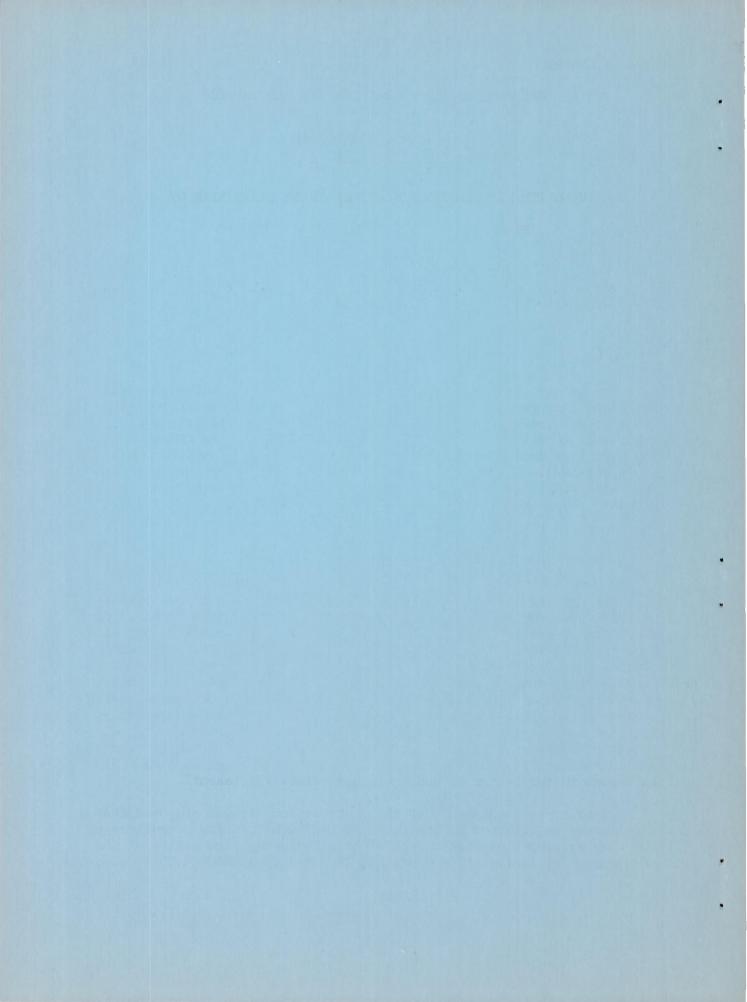
By Leland B. Salters, Jr.

Langley Aeronautical Laboratory
Langley Field, Va.

NATIONAL ADVISORY COMMITTEE FOR AERONAUTICS

WASHINGTON

June 21, 1955



NATIONAL ADVISORY COMMITTEE FOR AERONAUTICS

RESEARCH MEMORANDUM

VELOCITY DISTRIBUTIONS MEASURED IN THE SLIPSTREAM OF

EIGHT-BLADE AND SIX-BLADE DUAL-ROTATING

PROPELLERS AT ZERO ADVANCE

By Leland B. Salters, Jr.

SUMMARY

The nature of the slipstream of NACA 8.75-(5)(05)-037 eight- and six-blade dual-rotating propellers has been investigated under static conditions. The slipstream-boundary cone angle was found to agree qualitatively with the theoretical angle of spread for an unheated jet. The magnitude and direction of the slipstream rotation varied with blade-angle settings. The geometrical shape of the slipstream was found to vary with time, the maximum recorded radial shift in position of the boundary being one-fourth the propeller diameter.

INTRODUCTION

The growing interest of the aircraft industry in vertical-takeoff aircraft powered by dual-rotating propellers has increased the need for knowledge of the nature of the slipstream of the dual-rotating propeller. Some types of vertical-takeoff aircraft at zero or low forward speed depend, for longitudinal and directional control, upon the action of the slipstream on control surfaces immersed in the slipstream. In order to obtain the proper design of such surfaces, a knowledge of the characteristics of the slipstream behind a dual-rotating propeller is necessary. Although there are some data available on the characteristics of dual-rotating propeller slipstreams at high forward speeds, there are very little data available for the condition at zero advance, such as would be needed in the design of convertible aircraft for takeoff.

In order to supply some of this information, it was proposed that a wake survey be obtained during tests of two dual-rotating propellers at the Langley propeller static test stand. These tests consisted of the measurement of forces and vibrational stresses on an NACA 8.75-(5)(05)-037

dual-rotating propeller. Therefore, a survey of the slipstream which consisted of a longitudinal survey from 0.23 to 3.77 propeller diameters behind the propeller and a stationary survey at the 1.60-diameter station was included in the test program.

The survey was made with a single rake extending vertically from outside the slipstream down to the center or inner boundary of the slipstream. Although only a part of the wake was covered by the rake, it is believed to represent a fair average of the whole wake. The longitudinal survey was made at a constant rotational speed of 1,000 rpm for front-unit blade angles from 8° to 28° at 0.75 tip radius. The stationary survey was made for front-unit blade angles, at the 0.75 radial station, from 4° to 36° and for rotational speeds from 600 to 2,200 rpm, except where the rotational speeds were limited to lower values due to propeller flutter.

SYMBOLS

Ъ	blade width, ft
В	number of blades
cld	design section lift coefficient
C _P	power coefficient, $\frac{P}{\rho n^3 D^5}$
${\tt C}_{ m T}$	thrust coefficient, $\frac{T}{\rho n^2 D^4}$
D	propeller diameter, ft
h	blade section maximum thickness, ft
n	propeller rotational speed, rps
P	power, ft-lb/sec
p	static pressure, lb/sq ft
r	radius to blade element, ft
R	propeller tip radius, ft
T	thrust, 1b

V_s velocity of slipstream, fps

 V_{m} rotational tip speed, fps

β blade angle, deg

 $\beta_{0.75R}$ blade angle at 0.75 tip radius, deg

ρ air density, slugs/cu ft

Subscripts:

F front

R rear

APPARATUS

<u>Propeller</u>.- An NACA 8.75-(5)(05)-037 dual-rotating propeller having NACA 16-series sections was used with the Langley 6,000-horsepower propeller dynamometer as described in reference 1 and shown in figure 1. Blade-form curves are given in figure 2. The propeller was tested in both the eight- and six-blade configurations, the front and rear units of the propeller being spaced $13\frac{1}{8}$ inches apart. The activity factor per blade was 114.32; therefore, it was 914.56 for the eight-blade configuration and 685.92 for the six-blade configuration.

Survey rakes. - The two rakes shown in figure 1 were used in the investigation. For the longitudinal survey, a rake was mounted vertically on a mobile crane which permitted an axial movement from 2 to 33 feet behind the propeller. The second rake was fixed to the side of the dynamometer at an angle of 1480 from the vertical and located 2 feet behind the propeller. Axial-station designations are referenced to the plane of rotation of the rear unit of the propeller.

TESTS

The NACA 8.75-(5)(05)-037 dual-rotating propeller was statistically tested at blade angles of 4°, 8°, 12°, 16°, 20°, 28°, and 36° and at rotational speeds from 600 to 2,200 rpm except where rotational speeds were

limited to smaller values due to critical blade stresses. The propeller was tested in both the eight- and six-blade configurations. A differential of 1° was maintained at r/R = 0.75 between the blade angles of the front and rear units, the front unit having the larger angles.

Longitudinal survey. Total and static-pressure measurements were taken at constant rotational speeds by the vertical rake at longitudinal stations located 2, 6, 10, 14, 22, 27, and 33 feet behind the rear unit of the propeller, which in the distance—propeller-diameter ratio covers a range from 0.23 to 3.77.

Stationary survey. Total and static-pressure measurements were made for the complete test program with the vertical rake located at the 1.60-diameter station. For some of the tests, like measurements were taken by the side rake located at the 0.23-diameter station.

RESULTS AND DISCUSSION

Longitudinal survey. The results of the longitudinal velocity survey of the slipstream from the 0.23- to 3.77-diameter stations are given in figure 3 for both the eight- and six-blade configurations, where the velocity ratio is also plotted against propeller radius for several axial distances behind the propeller. The rotational speed was maintained at 1,000 rpm and the blade angle at the 0.75 tip radius varied from 8° to 28°. From the 0.23- to 1.60-diameter stations, the vertical rake extended from outside the slipstream to within 1 inch of the dynamometer case and from the 2.52- to 3.77-diameter stations, to the dynamometer center line.

Some indication of the physical characteristics of the slipstream, such as the angle of spread and the velocity distribution, may be obtained from a study of these results; however, allowance must be made for the distortion of the flow streamlines due to the presence of the dynamometer case and fairings. The theoretical angle of spread for an unheated jet (ref. 2) is included for comparison. It may be observed that the spread of the slipstream agrees qualitatively with that of the jet from the point of minimum diameter of the slipstream to the end of the straight cylindrical part of the dynamometer shell. The disagreement downstream of this point may be attributed to the contraction of the streamlines due to the converging parts of the dynamometer shell.

Account must also be made of the nonsteady character of the slip-stream. The general shape of the slipstream did not remain fixed but varied with time, a phenomenon which will be discussed later. The possibility of radial nonsymmetry of the slipstream about the propeller axis must also be considered, although it is believed that the survey of a part of the slipstream will, over a period of time, give a fair average of the complete slipstream.

NACA RM L55D21 5

Stationary survey. In order to determine the effects of variations in propeller blade angle and rotational speed upon velocity distributions at a typical station in the slipstream, the vertical rake was located at the 1.60-diameter station for a series of tests. The results of these tests are given in figures 4 and 5 where velocity ratio is plotted against fraction of tip radius for ranges of rotational speed and blade angle. In considering these figures, one of the most noticeable features is the pronounced variation in velocity distribution in slipstream, both as to shape of the curves and the extent of the boundaries. The boundary of the slipstream, as indicated by these curves, varied over wide limits. These differences cannot be attributed to variations in rotational speed nor blade angle but rather to the variation of the slipstream characteristics with time.

One of the unexpected findings of these tests was that the slipstream, ordinarily thought of as a stable, steady flow, was actually shifting in position and velocity distribution continually. The maximum shift in position of the boundary recorded in these tests amounted to one-fourth the propeller diameter. The slipstream was found to writhe, twist, and distort with or without side winds or gusts. The transition from one shape to another was not always continuous; quite often the boundaries would retain one shape for a period of 5 to 20 seconds and then shift to another shape and remain fixed in the new configuration for a similar period of time and so forth. It has not been determined whether the distortion of the boundary is due to lateral shift of the whole slipstream, to distortion of the cross-sectional shape of the slipstream, or to both.

The limits of accuracy in the reading of the film from photographs of the manometer board was 0.05 inch of alcohol. All points above this limit are included in these plots. The point for zero velocity could not be determined because of the extreme sensitivity of the velocity to even minute changes in dynamic pressure near the lower limits. However, the curves were extrapolated to the zero line by extending the curves beyond the last point with the shape before the last point being used as a criterion.

A complete coverage of the rotational speeds and blade-angle settings could not be obtained due to the limitations in blade stresses caused by propeller flutter.

Effect of blade angle. Figure 6 shows the effect of blade angle upon the velocity distribution in the slipstream at the 1.60-diameter station for the eight- and six-blade configurations at 800 rpm. In general, the spread of the slipstream, as well as the magnitude of the velocity, increases with increase in blade angle over the range of rotational speed included in these tests.

Nature of flow near propeller .- In figure 7 are presented the results of a velocity survey of the eight-blade dual-rotating propeller slipstream as measured at the 0.23-diameter station at a blade-angle setting of 80 (front unit) for various rotational speeds. The diagram is to scale and shows the rake in its position relative to the propeller. The dashed lines represent the slipstream boundaries of the front and rear units of the propeller, the spread in the dashed lines representing the shift in the wake. It may be observed that the part of the slipstream below the front-unit boundary has been acted upon by both units, whereas that part above the front-unit boundary has been acted upon by only the rear blades. This is believed to account for the sudden break in the velocity-distribution curves, the lower part having the greater velocities. This break is clearly defined only in the case of the lower blade angles and at stations near the propeller. At greater distances from the propeller and at higher blade angles, the break is obscured by the greater turbulence in the slipstream associated with these conditions.

Effect of blade angle on slipstream rotation. It was observed that the ratio of power absorbed by the front and rear units of the propeller varied with the blade-angle settings. At low blade angles the front unit absorbed more power than the rear unit, but at high blade angles the rear unit absorbed the greater power. A plot of power coefficient $C_{\rm p}$ against blade angle $\beta_{\rm O.75R}$ is included as figure 8. From this it may be concluded that the magnitude and direction of the net rotation of the slipstream varied with blade-angle settings.

CONCLUDING REMARKS

An investigation into the nature of the slipstream of dual-rotating propellers has revealed several interesting facts.

The slipstream-boundary cone angle was found to agree qualitatively with the theoretical angle of spread for an unheated jet along the straight part of the dynamometer shell.

The shape of the slipstream boundary was found to vary with time. Under similar conditions, large variations were observed in the lateral position of the elements of the boundary and lateral displacements up to 25 percent of the propeller diameter were recorded.

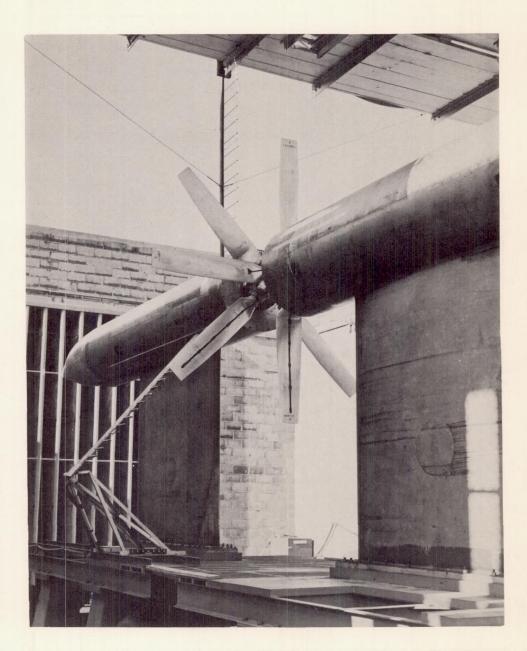
NACA RM L55D21 7

The magnitude and direction of the slipstream rotation were found to vary with blade-angle settings.

Langley Aeronautical Laboratory,
National Advisory Committee for Aeronautics,
Langley Field, Va., March 30, 1955.

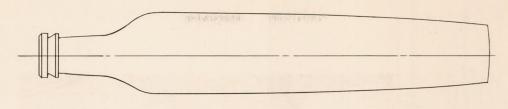
REFERENCES

- 1. Wood, John H., and Swihart, John M.: The Effect of Blade-Section Camber on the Static Characteristics of Three NACA Propellers. NACA RM L51L28, 1952.
- 2. Kuethe, Arnold M.: Investigations of the Turbulent Mixing Regions Formed by Jets. Jour. Appl. Mech., vol. 2, no. 3, Sept. 1935, pp. A-87 A-95.



L-78831

Figure 1.- NACA 8.75-(5)(05)-037 dual-rotating propeller mounted on Langley 6,000-horsepower propeller dynamometer with survey rakes installed.



Developed plan form

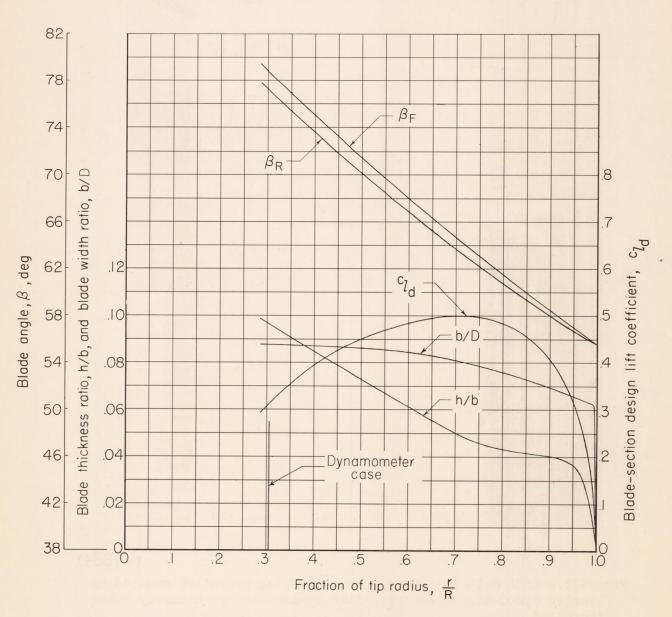


Figure 2.- Blade-form curves and developed plan form for NACA 8.75-(5)(05)-037 dual-rotating propeller.

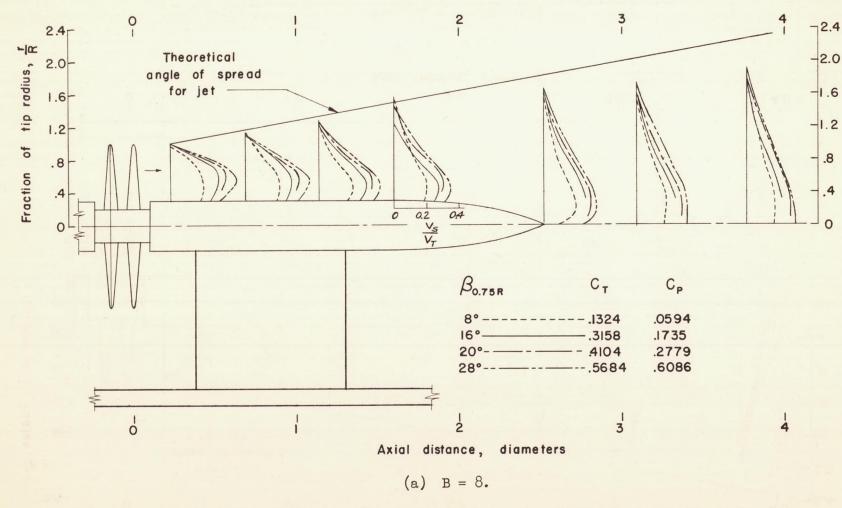


Figure 3.- Schematic view of dynamometer and longitudinal survey of slipstream of dual-rotating propellers at 1,000 rpm.

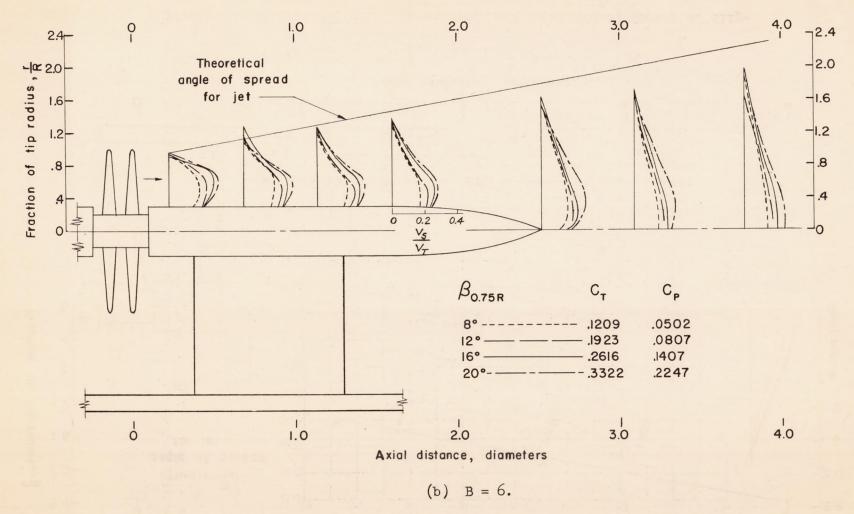


Figure 3. - Concluded.

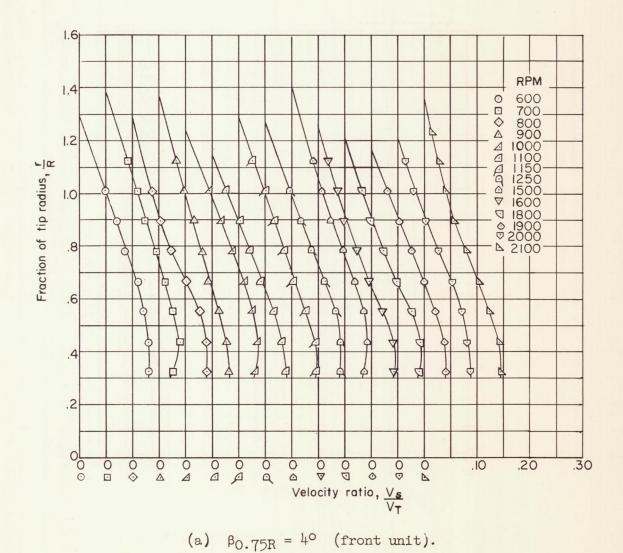
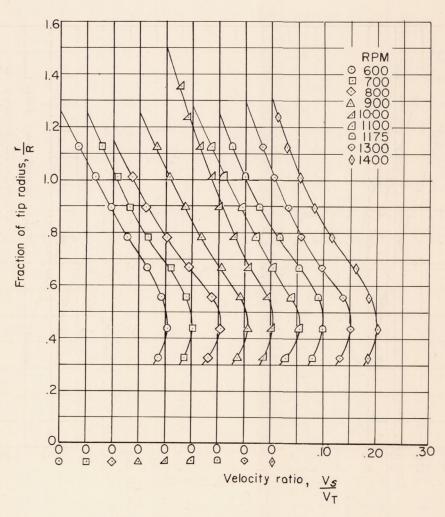
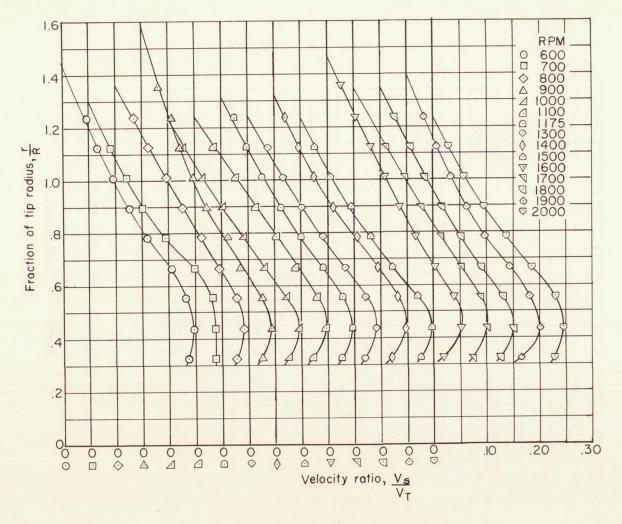


Figure 4.- Velocity distribution in slipstream at 1.60-diameter station for eight-blade dual-rotating propeller at various rotational speeds.



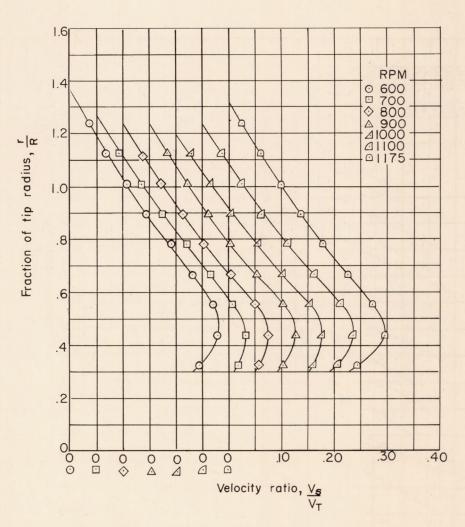
(b) $\beta_{0.75R} = 8^{\circ}$ (front unit).

Figure 4. - Continued.



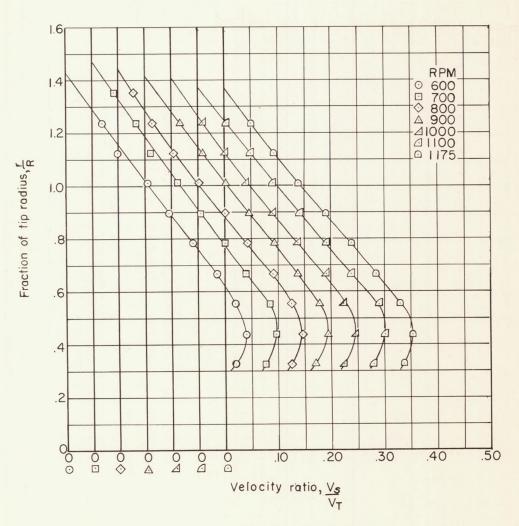
(c)
$$\beta_{0.75R} = 12^{\circ}$$
 (front unit).

Figure 4. - Continued.



(d) $\beta_{0.75R} = 16^{\circ}$ (front unit).

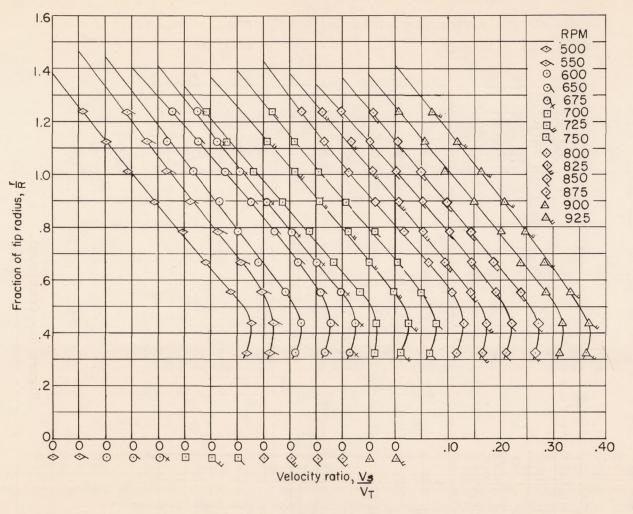
Figure 4. - Continued.



(e) $\beta_{0.75R} = 28^{\circ}$ (front unit).

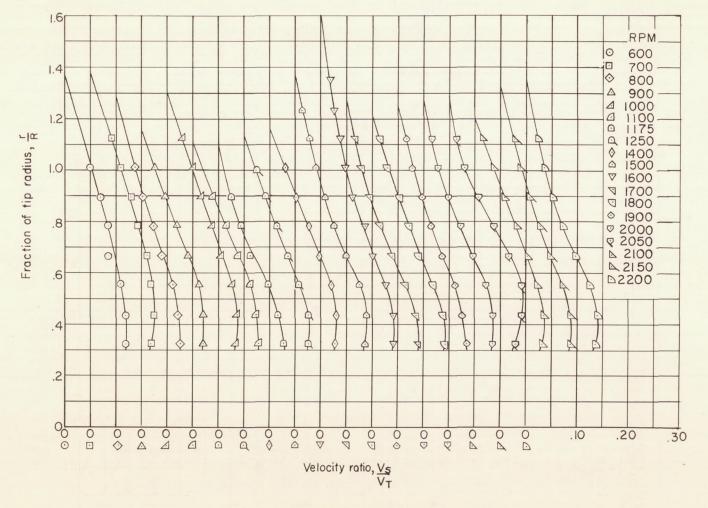
Figure 4.- Continued.

Y



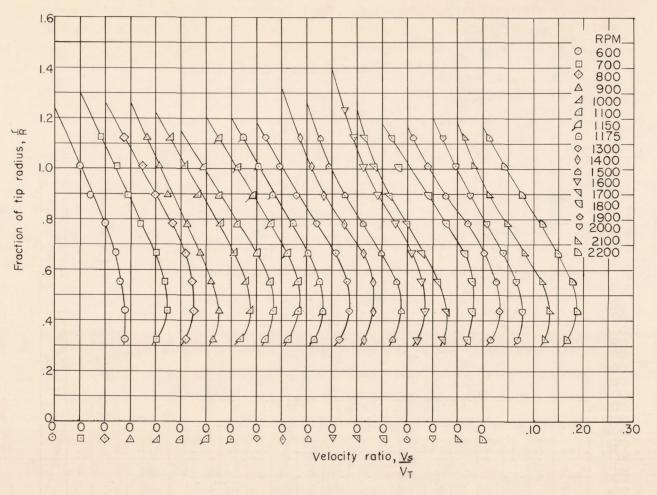
(f) $\beta_{0.75R} = 36^{\circ}$ (front unit).

Figure 4. - Concluded.



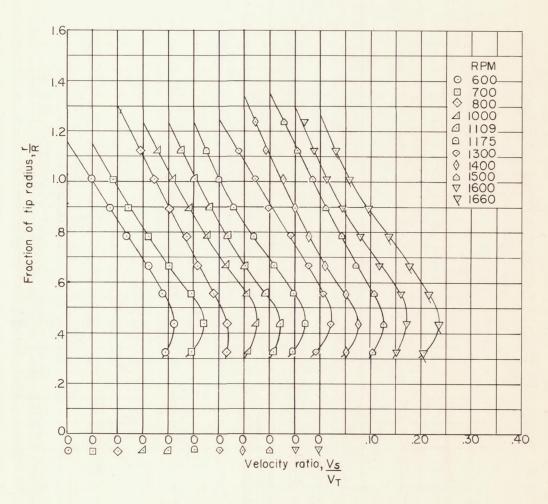
(a) $\beta_{0.75R} = 4^{\circ}$ (front unit).

Figure 5.- Velocity distribution in slipstream at 1.60-diameter station for six-blade dual-rotating propeller at various rotational speeds.



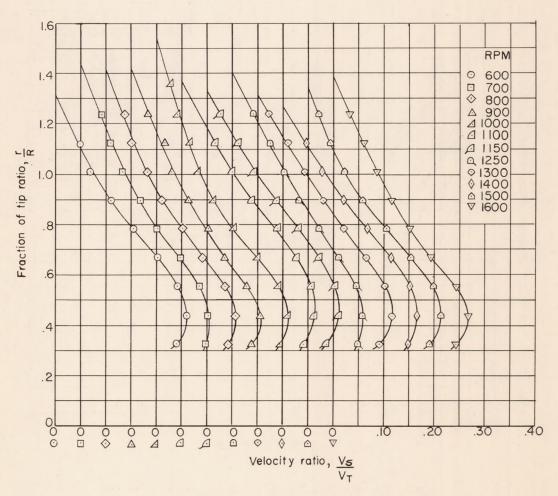
(b) $\beta_{0.75R} = 8^{\circ}$ (front unit).

Figure 5. - Continued.



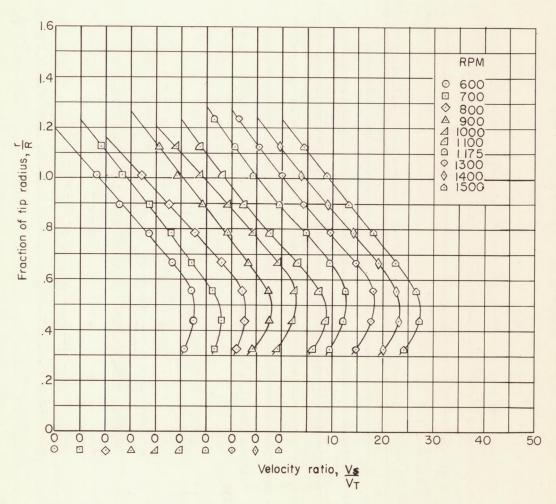
(c) $\beta_{0.75R} = 12^{\circ}$ (front unit).

Figure 5.- Continued.



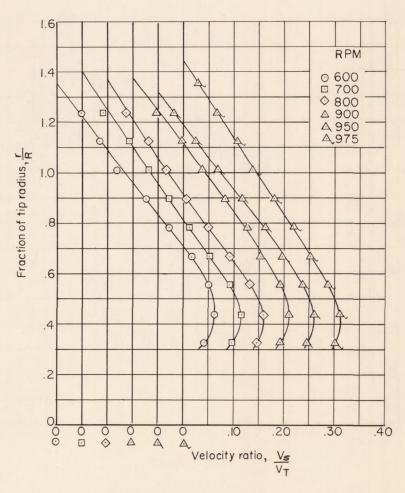
(d) $\beta_{0.75R} = 16^{\circ}$ (front unit).

Figure 5. - Continued.



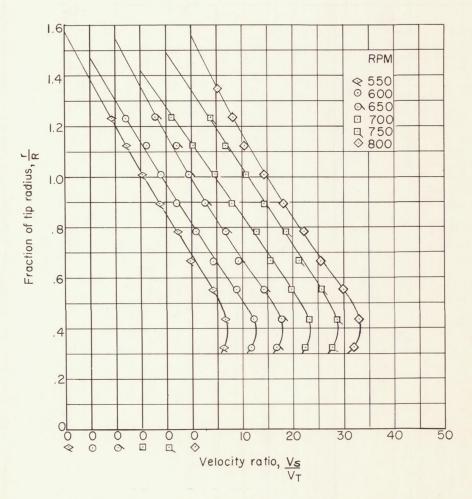
(e) $\beta_{0.75R} = 20^{\circ}$ (front unit).

Figure 5. - Continued.



(f) $\beta_{0.75R} = 28^{\circ}$ (front unit).

Figure 5. - Continued.



(g) $\beta_{0.75R} = 36^{\circ}$ (front unit).

Figure 5. - Concluded.

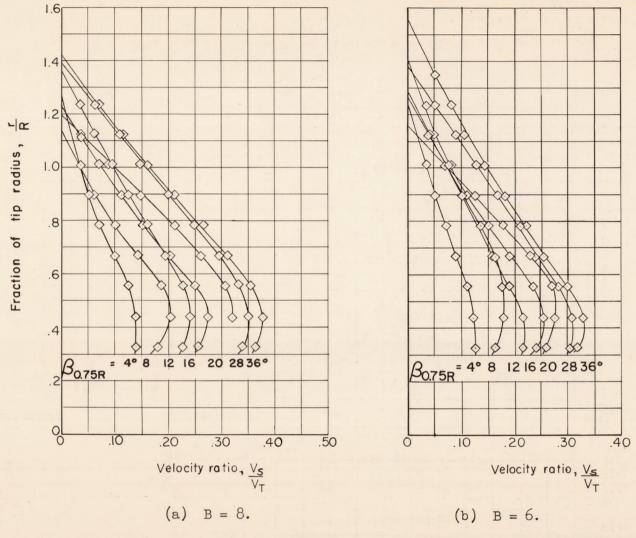


Figure 6.- Comparison of velocity distributions in slipstream at 1.60-diameter station at various blade-angle settings at 800 rpm.

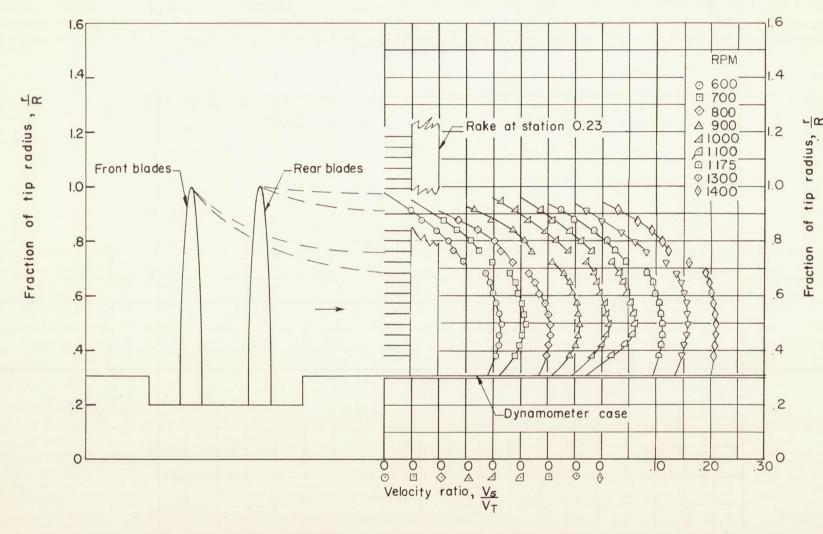


Figure 7.- Nature of flow in slipstream of dual-rotating propeller for static conditions at various rotational speeds. $\beta_{0.75R} = 8^{\circ}$ (front unit); B = 8.

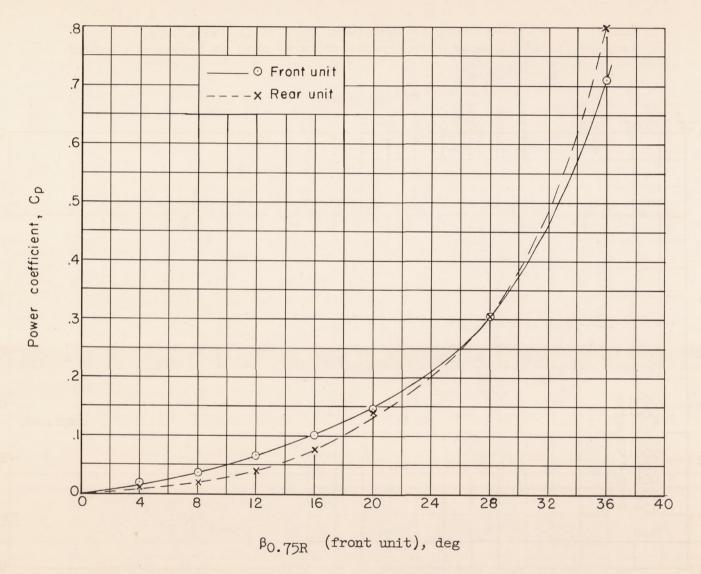


Figure 8.- Comparison of power coefficients of front and rear units of eight-blade dual-rotating propeller over a range of blade angle.